Journal of Hazardous Materials B125 (2005) 121–129

Journal of Hazardous Materials

www.elsevier.com/locate/jhazmat

Batch and column studies on biosorption of acid dyes on fresh water macro alga *Azolla filiculoides*

T.V.N. Padmesh [a], K. Vijayaraghavan [a], G. Sekaran [b], M. Velan [a,*]

[a] *Department of Chemical Engineering, Anna University, Chennai 600025, India*
[b] *Department of Environmental Technology, Central Leather Research Institute, Chennai 600020, India*

Received 21 January 2005; accepted 12 May 2005
Available online 13 June 2005

Abstract

The biosorption of Acid red 88 (AR88), Acid green 3 (AG3) and Acid orange 7 (AO7) by deactivated fresh water macro alga *Azolla filiculoides* was investigated in batch mode. Langmuir and Freundlich adsorption models were used for the mathematical description of the batch biosorption equilibrium data and model constants were evaluated. The adsorption capacity was pH dependent with a maximum value of 109.0 mg/g at pH 7 for AR88, 133.5 mg/g at pH 3 for AG3 and 109.6 mg/g at pH 3 for AO7, respectively, was obtained. The pseudo first and second order kinetic models were also applied to the experimental kinetic data and high correlation coefficients favor pseudo second order model for the present systems. The ability of *A. filiculoides* to biosorb AG3 in packed column was also investigated. The column experiments were conducted to study the effect of important design parameters such as initial dye concentration (50–100 mg/L), bed height (15–25 cm) and flow rate (5–15 mL/min) to the well-adsorbed dye. At optimum bed height (25 cm), flow rate (5 mL/min) and initial dye concentration (100 mg/L), *A. filiculoides* exhibited 28.1 mg/g for AG3. The Bed Depth Service Time model and the Thomas model were used to analyze the experimental data and the model parameters were evaluated.

Keywords: Biosorption; Acid red 88; Acid green 3; Acid orange 7; *Azolla filiculoides*; Packed column

1. Introduction

Pollution control is one of the prime concerns of society today. Untreated or partially treated wastewaters and industrial effluent discharges into natural ecosystems pose a serious problem to the environment [1]. Among industrial wastewaters, dye wastewater from textile and dyestuff industries is one of the most difficult waters to treat. This is because dyes usually have a synthetic and complex aromatic molecular structure, which makes them more stable and have difficult to biodegrade [2,3]. The dyes used in the textile industries include several structural varieties such as acidic, reactive, basic, disperse, azo, diazo, anthraquinone based and metal complex dyes [4]. A number of processes, like flocculation, chemical coagulation, precipitation [5], ozonation [6] and adsorption [7] have been employed for the treatment of dye bearing wastewaters. Although the above said physical and/or chemical methods have been widely used, they possess inherent limitations such as high cost, formation of hazardous byproducts and intensive energy requirements [8].

Biological processes such as biosorption [9], bioaccumulation [10] and biodegradation [11] have been proposed as having potential application in removal of dyes from textile wastewater. Among these, biosorption is more advantageous for water treatment because in this process, dead organisms are not affected by toxic wastes, they do not require a continuous supply of nutrients and they can be regenerated and reused for many cycles [12].

Dead bacteria, yeast and fungi have all been used for the purpose of decolorizing dye-containing wastewater [13]. Limited numbers of studies are available on the biological treatment by algal species [8,14,15], in spite of their ubiquitous distribution and their central role in the fixation and

* Corresponding author. Tel.: +91 44 22203506; fax: +91 44 22352642.
E-mail address: velan@annauniv.edu (M. Velan).

0304-3894/$ – see front matter © 2005 Elsevier B.V. All rights reserved.
doi:10.1016/j.jhazmat.2005.05.014

turnover of carbon and other nutrient elements [16]. In particular, no research attention has been focused on utilization of macro algae for dye removal. Macro fresh water algae, a renewable natural biomass proliferates ubiquitously and abundantly in the many parts of the world. *Azolla filiculoides*, a fresh water blue green alga, has been shown to effectively bind chromium [17], zinc [18] and nickel [19] in aqueous solutions. This alga is commonly found in ditches, ponds and slow moving streams and is capable of colonizing rapidly to form dense mats over water surfaces thus imposing negative effects on the aquatic ecology [18]. Thus, its usage in wastewater treatment is of interest and it may also add revenue to the local community. Furthermore, its macroscopic structure and rigid shape is particularly suitable for biosorption column applications.

The present work investigated the dye biosorption behavior of *A. filiculoides* using Acid red 88 (AR88), Acid green 3 (AG3) and Acid orange 7 (AO7) as model acid dyes.

2. Materials and methods

2.1. Azolla filiculoides

A. filiculoides was collected from Milk Producers Union, Tirunelveli, India. It was sun dried then crushed and finally sieved to particle sizes in the range of 1–2 mm. The biomass was then treated with 0.1 M HCl for 5 h followed by washing with distilled water and then dried in shade. The resultant biomass was subsequently used in sorption experiments.

2.2. Dyes and their structures

Acid red 88, Acid green 3 and Acid orange 7 were obtained from Sigma–Aldrich Corporation, Bangalore, India. The properties of the dyes used are given in Table 1. The chemical structures of all three acid dyes are shown in Fig. 1.

2.3. Batch experiments

Batch biosorption experiments were performed in a rotary shaker at 150 rpm using 250 mL Erlenmeyer flasks containing 0.2 g *Azolla* biomass in 50 mL of solution containing different acid dye concentrations at desired pH conditions (using 0.1 M HCl and 0.1 M NaOH). After 12 h, the reaction mixture was centrifuged at 3000 rpm for 10 min. The dye content in the supernatant was determined using UV-Spectrophotometer (Hitachi, Japan) at respective λ_{max} values shown in Table 1. The amount of dye biosorbed was calculated from the differences between the dye quantity added to the biomass and the dye content of the supernatant using the following equation:

Table 1
Properties of the dyes

C.I. name	Molecular weight	λ_{max} (nm)	Molecular formula
Acid red 88	400.39	503	$C_{20}H_{13}N_2NaO_4S$
Acid green 3	690.82	636	$C_{37}H_{37}N_2O_6S_2Na$
Acid orange 7	350.33	452	$C_{16}H_{11}N_2NaO_4S$

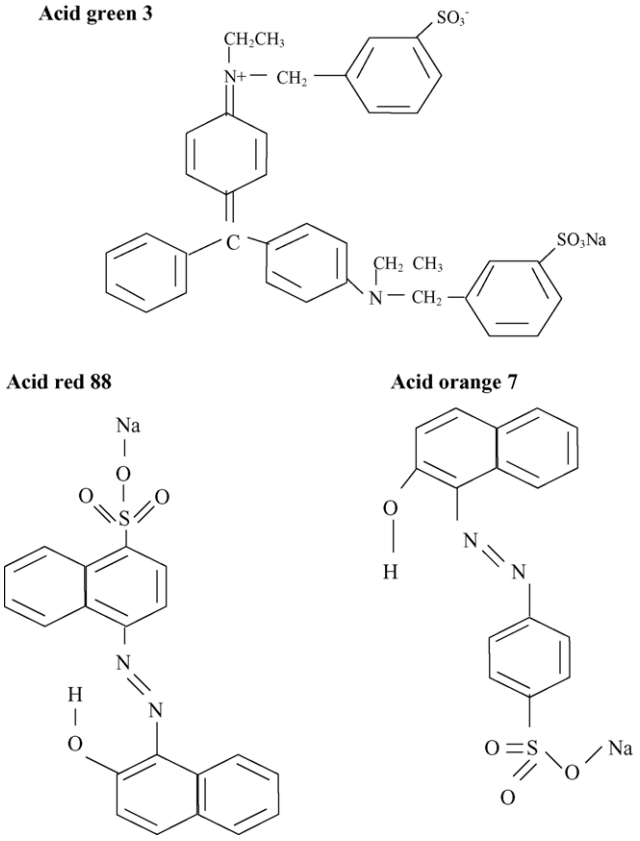

Fig. 1. The chemical structures of three acid dyes used in this study.

$$q_e = \frac{(C_0 - C_e) \times V}{M} \quad (1)$$

where q_e is the dye uptake (mg/g), C_0 and C_e the initial and equilibrium dye concentrations in the solution (mg/L), respectively, V the solution volume (L) and M is the mass of biosorbent (g).

For kinetic experiments, samples were taken at regular time intervals and analyzed for dye concentration. To evaluate the differences in the biosorption rates and uptakes, the kinetic data were described with pseudo first and pseudo second order models. The linearized form of pseudo first and pseudo second order model [7] are shown below as Eqs. (2) and (3), respectively:

$$\log(q_e - q_t) = \log(q_e) - \frac{k_1}{2.303}t \quad (2)$$

$$\frac{t}{q_t} = \frac{1}{k_2 q_e^2} + \frac{1}{q_e}t \quad (3)$$

where q_t is the amount of dye sorbed at time t (mg/g), k_1 the first order rate constant (1/min) and k_2 is the second order rate constant (g/(mg min)).

2.4. Column experiments

Continuous flow sorption experiments were conducted in a glass column (2 cm internal diameter and 35 cm height). At the top of the column; an adjustable plunger was attached with a 0.5 mm stainless sieve. At the bottom of the column, a 0.5 mm stainless sieve was attached followed by glass wool. A 2 cm high layer of glass beads (1.5 mm in diameter) was placed at the column base in order to provide a uniform inlet flow of the solution into the column.

A known quantity of *A. filiculoides* was packed in the column to yield the desired bed height of the sorbent. Dye solution of known concentration was pumped upward through the column at a desired flow rate by a peristaltic pump (Miclins). The concentration of dye at the vent of the column was collected at regular time intervals. All batch and continuous experiments were conducted at room temperature (30 °C).

The breakthrough time (t_b, the time at which dye concentration in the effluent reached 1 mg/L) and bed exhaustion time (t_e, the time at which dye concentration in the effluent reached 100 mg/L) were used to evaluate the breakthrough curves. The slope of the breakthrough curve (dc/dt) was determined from t_b to t_e. The total quantity of dye mass biosorbed in the column (m_{ad}) is calculated from the area above the breakthrough curve (outlet dye concentration (C) versus time (t)) multiplied by the flow rate. Dividing the dye mass (m_{ad}) by the sorbent mass (M) leads to the uptake capacity (Q) of the alga [20]. Effluent volume (V_{eff}) can be calculated as follows [21]:

$$V_{eff} = F \cdot t_e \times \frac{60}{1000} \tag{4}$$

where F is the volumetric flow rate (mL/min).

Total amount dye sent to column (m_{total}) can be calculated as follows [21]:

$$m_{total} = \frac{C_0 F t_e}{1000} \tag{5}$$

where C_0 is the inlet dye concentration (mg/L).

Total dye removal percent with respect to flow volume can be calculated as follows [21]:

$$\text{total dye removal (\%)} = \frac{m_{ad}}{m_{total}} \times 100 \tag{6}$$

2.5. Modeling of column data

BDST is a simple model, which states that bed height (Z) and service time (t) of a column bears a linear relationship. The equation can be expressed as [22]:

$$t = \frac{N_0 Z}{C_0 v} - \frac{1}{K_a C_0} \ln\left(\frac{C_0}{C_b} - 1\right) \tag{7}$$

where C_b is the breakthrough dye concentration (mg/L), N_0 the sorption capacity of bed (mg/L), v the linear velocity (cm/h) and K_a is the rate constant (L/(mg h)).

The column biosorption data obtained at different bed heights, flow rates and dye concentrations were fitted using the Thomas model. The linearized form of Thomas model can be expressed as follows [23]:

$$\ln\left(\frac{C_0}{C} - 1\right) = \frac{k_{Th} Q_0 M}{F} - \frac{k_{Th} C_0}{F} V \tag{8}$$

where k_{Th} is the Thomas model constant (L/mg h), Q_0 the maximum solid-phase concentration of solute (mg/g) and V is the throughput volume (L). The model constants k_{Th} and Q_0 can be determined from a plot of $\ln[(C_0/C) - 1]$ against t [21].

3. Results and discussion

3.1. Batch studies

3.1.1. Effect of pH and initial dye concentration

The pH value of the solution is an important controlling parameter in the adsorption process, and the initial pH value of the solution has more influence than the final pH, which influences both the cell surface dye binding sites and the dye chemistry in water [24]. The effect of pH on dye uptake in the batch process was studied by varying the pH from 2 to 7 (Fig. 2). For each pH value, the dye concentrations were varied from 10 to 1000 mg/L. The biosorbent dosage (4 g/L) and agitation speed (150 rpm) were kept constant. *Azolla* biomass exhibited high AR88 uptakes in the pH range of 6–7, whereas it biosorbed more AG3 and AO7 in the pH range of 2–3. Also, at all pH conditions examined, the isotherm curve become smooth and approached the plateau value at higher dye concentrations. The plateau region of the isotherm represents well-packed dye molecules covering the total surface area of the biosorbent [25].

The equilibrium biosorption data can be modeled by using simple adsorption models such as Langmuir (Eq. (9)) and Freundlich (Eq. (10)) models:

$$q_e = \frac{q_{max} b C_e}{1 + b C_e} \tag{9}$$

$$q_e = K_F C_e^{1/n} \tag{10}$$

where q_{max} is the maximum dye uptake (mg/g), b the Langmuir equilibrium constant (L/mg), K_F the Freundlich constant $(L/g)^{1/n}$ and n is the Freundlich affinity constant. The main reason for the extended use of these isotherms is that they incorporate constants that are easily interpretable. All the model parameters were evaluated by non-linear regression and summarized in Table 2.

Langmuir sorption model [26] served to estimate the maximum dye uptake values where they could not be reached in the experiments. The constant b represents affinity between the sorbent and sorbate. The Langmuir model parameters were largely dependent on the initial solution pH. For AR88, both q_{max} and b increases with increasing initial solution pH

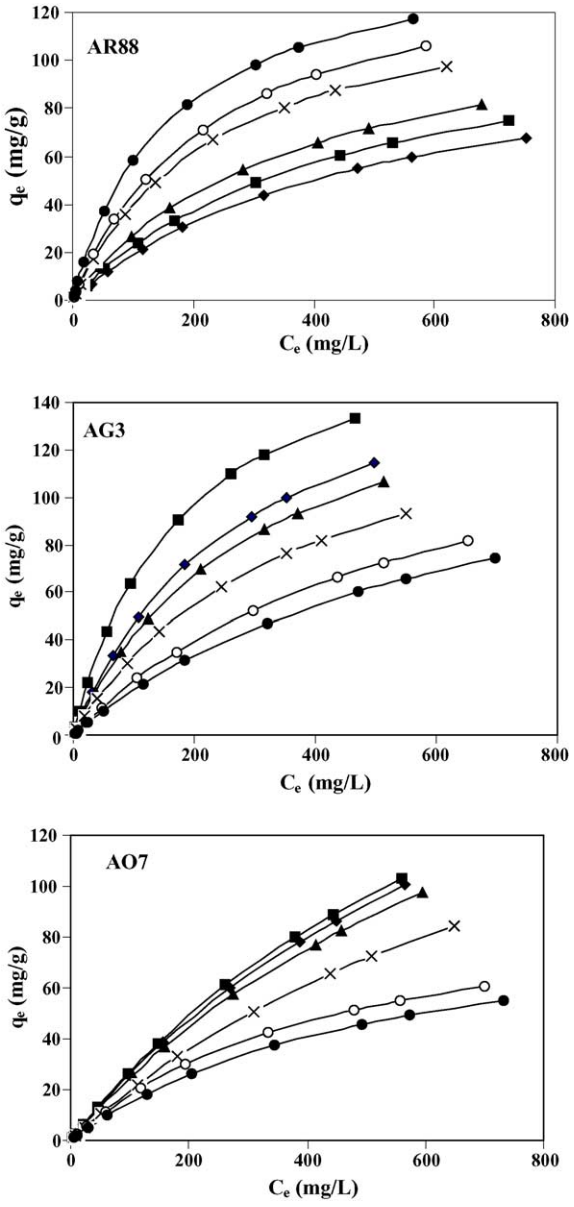

Fig. 2. Sorption isotherms of different azo dyes by *A. filiculoides* at different pH conditions (M = 4 g/L, agitation speed = 150 rpm). (♦) pH 2; (■) pH 3; (▲) pH 4; (×) pH 5; (◯) pH 6; (●) pH 7.

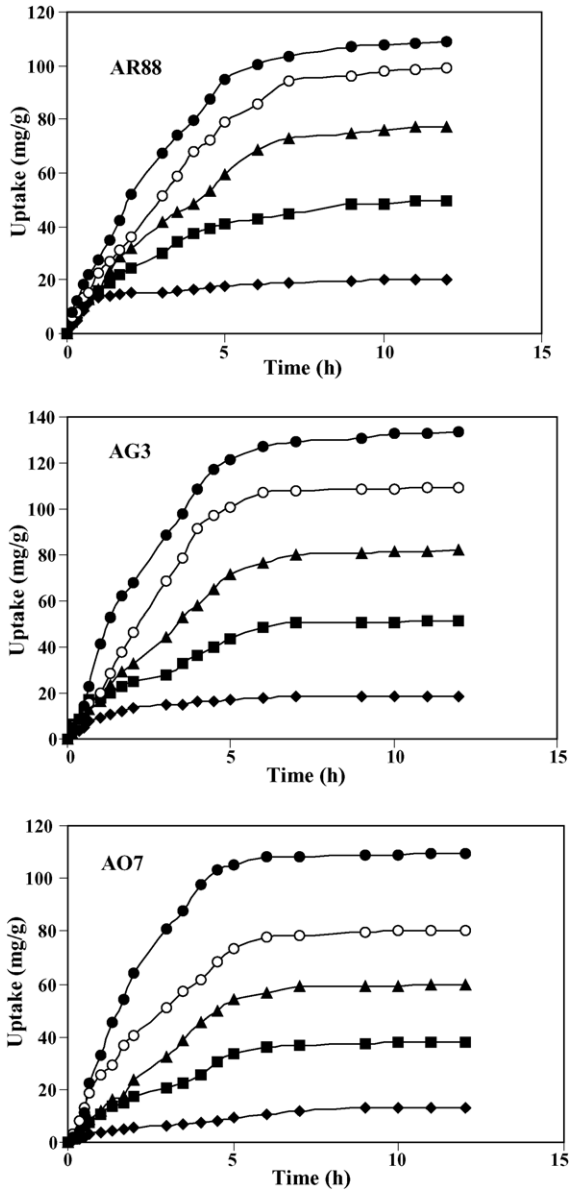

Fig. 3. Effect of initial acid dye concentrations on the biosorption potential of *A. filiculoides*. (♦) 100 mg/L; (■) 300 mg/L; (▲) 500 mg/L; (◯) 700 mg/L; (●) 1000 mg/L.

and reached maximum at pH 7. In contrast, for AG3 and AO7, the Langmuir constants exhibited high values at low pH (pH 3) and decreased as the pH increased. High values of b were reflected in the steep initial slope of a sorption isotherm, indicating desirable high affinity. Thus, for good biosorbents in general, high q_{max} and a steep initial isotherm slope (i.e. high b) are desirable. The Freundlich equation [27] is an empirical equation employed to describe the heterogeneous systems. It is worth noting that both Freundlich constants (K_F and n) also reached their maximum values at pH 7 for AR88 and at pH 3 for both AG3 and AO7. This implies that the binding capacity reaches the highest value and the affinity between the biomass and dye was also higher than other pH values investigated.

3.1.2. Batch kinetic studies

The experimental results of biosorption of acid dyes on *A. filiculoides* at various initial concentrations are shown in Fig. 3. For all dyes, biosorption rate was slow and also the equilibrium time attainment increased with increasing dye concentration. On increasing the initial dye concentrations, the total dye uptake increased and the total percent removal decreased. For instance, on changing initial AR88 concentrations from 10 to 1000 mg/L, the amount sorbed increased from 2.04 to 109 mg/g at pH 7. But the removal efficiency decreased from 81.7 to 43.6% as the AR88 concentration increases from 10 to 1000 mg/L. This is because at lower concentration, the ratio of the initial moles of dye molecules

Table 2
Langmuir and Freundlich model parameters at different pH conditions

Dye	pH	Langmuir parameters			Freundlich parameters		
		q_{max} (mg/g)	b (L/mg)	$R^{2\dagger}$	K_F (L/g)$^{1/n}$	n	$R^{2\dagger}$
AR88	2.0	73.5	0.0029	0.994	0.355	1.22	0.987
	3.0	88.5	0.0034	0.999	0.516	1.28	0.992
	4.0	95.2	0.0044	0.992	0.710	1.32	0.994
	5.0	106.4	0.0064	0.998	1.066	1.36	0.986
	6.0	117.7	0.0068	0.997	1.260	1.36	0.986
	7.0	123.5	0.0091	0.997	1.654	1.39	0.963
AG3	2.0	126.6	0.0038	0.988	0.589	1.10	0.979
	3.0	137.0	0.0052	0.992	0.964	1.16	0.970
	4.0	133.3	0.0039	0.995	0.617	1.08	0.977
	5.0	121.9	0.0021	0.999	0.211	0.94	0.985
	6.0	114.9	0.0011	0.991	0.068	0.82	0.981
	7.0	109.9	0.0010	0.990	0.055	0.81	0.981
AO7	2.0	108.3	0.0034	0.999	0.434	1.18	0.999
	3.0	109.6	0.0043	0.992	0.505	1.23	0.999
	4.0	100.9	0.0041	0.998	0.468	1.20	0.997
	5.0	87.8	0.0040	0.998	0.462	1.19	0.999
	6.0	74.8	0.0030	0.999	0.338	1.17	0.999
	7.0	67.1	0.0028	0.999	0.275	1.15	0.999

† Correlation coefficient.

to the available surface area is low and subsequently the fractional sorption becomes independent of initial concentration. However, at higher concentration the available sites of sorption became fewer compared to the moles of dye present and hence the percentage dye removal is dependent upon the initial dye concentration.

In order to obtain the rate constants and equilibrium dye uptake, the straight-line plots of $\log(q_e - q_t)$ against t of Eq. (2) were made for *A. filiculoides* at different initial dye concentrations (Figure not presented). The intercept of the above plot should be equal to $\log q_e$. However, if the intercept does not equal the experimental equilibrium dye uptake then the reaction is not likely to be first order even though this plot has high correlation coefficient with the experimental data [28]. The rate constants, predicted equilibrium uptakes and the corresponding correlation coefficients for all concentrations tested have been calculated and summarized in Table 3. For all three dyes, correlation coefficients were found to be above 0.821, but the calculated q_e is not equal to experimental q_e, suggesting the insufficiency of pseudo first order model to fit the kinetic data for the initial concentrations examined. The reason for these differences in the q_e values is that there is a time lag, possibly due to a boundary layer or external resistance controlling at the beginning of the sorption process [7].

The pseudo second order model is based on the sorption capacity on the solid phase. Contrary to other well-established models, it predicts the behavior over the whole range of studies and it is in agreement with the chemisorption mechanism being the rate-controlling step [7]. This was consistent with the better results obtained with the pseudo second order model (Table 3). Correlation coefficients were always greater than 0.99 and the lowest correlation coefficient in this case was better than the first order model correlation coefficients. The values of predicted equilibrium sorption capacities showed good agreement with the experimental equilibrium uptake values.

The batch experimental results revealed that *A. filiculoides* performed relatively well on all three acid dyes. The biosorption performance of *A. filiculoides* decreased in the following sequence: AG3 > AR88 > AO7. Therefore, AG3 was further selected for examining the performance of *Azolla* biomass in packed column.

3.2. Column studies

3.2.1. Effect of bed height

In the initial stage of continuous experiments in column packed with *A. filiculoides*, the bed height was varied from 15 to 25 cm. In order to yield different bed heights, 6.12, 9.89 and 13.71 g of biomass were added to produce 15, 20 and 25 cm, respectively. The inlet dye concentration (100 mg/L) and the flow rate (5 mL/min) were kept constant. As shown in Fig. 4, both breakthrough and exhaustion time increased with increasing bed height, which resulted in a broadened mass transfer zone. The AG3 uptake capacity of the biomass was 50.3, 55.8 and 69.5 mg/g at bed heights of 15, 20 and 25 cm, respectively. High uptake was observed at the highest bed height due to an increase in the surface area of biosorbent, which provided more binding sites for the sorption [29,30]. Even though the breakthrough curves become steeper as the bed height decreased, indicated by high dc/dt values, a higher removal percentage was observed at the highest bed height (Table 4).

The BDST model is based on physically measuring the capacity of the bed at different breakthrough values. This

Table 3
Kinetic parameters for the dye biosorption onto *A. filiculoides* at different initial dye concentrations

Dye	Initial concentration (mg/L)	$(q_e)_{exp}$ (mg/g)	Pseudo first order			Pseudo second order		
			k_1 (1/min)	q_e (mg/g)	$R^{2\dagger}$	k_2 (g/(mg min))	q_e (mg/g)	$R^{2\dagger}$
AR88	100	20.3	0.511	19.4	0.882	0.0463	21.8	0.996
	300	49.6	0.450	76.8	0.911	0.0061	61.3	0.996
	500	76.1	0.450	106.0	0.945	0.0034	80.4	0.983
	700	99.2	0.448	135.9	0.956	0.0028	101.3	0.981
	1000	109.0	0.474	137.8	0.981	0.0027	109.9	0.990
AG3	100	19.3	0.573	15.4	0.984	0.0364	21.2	0.999
	300	55.1	0.526	67.8	0.951	0.0109	58.8	0.993
	500	85.5	0.558	125.1	0.954	0.0090	89.3	0.999
	700	109.5	0.562	145.8	0.976	0.0021	111.1	0.997
	1000	133.5	0.539	170.7	0.979	0.0014	135.1	0.998
AO7	100	13.4	0.484	20.9	0.894	0.0155	16.4	0.994
	300	37.9	0.594	59.8	0.945	0.0088	39.4	0.998
	500	59.5	0.690	108.7	0.980	0.0040	61.7	0.991
	700	80.2	0.590	111.8	0.975	0.0039	82.6	0.997
	1000	109.6	0.575	121.8	0.977	0.0037	112.4	0.995

† Correlation coefficient.

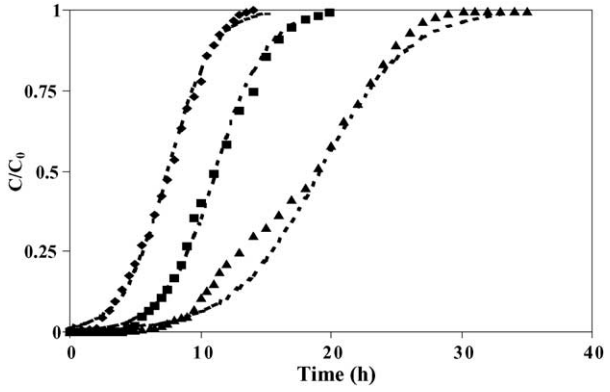

Fig. 4. Breakthrough curves for AG3 biosorption onto *A. filiculoides* biomass at different bed heights (flow rate = 5 mL/min, initial AG3 concentration = 100 mg/L, pH 3.0). Bed heights: (♦) 15 cm; (■) 20 cm; (▲) 25 cm. (- - -) Predicted from Thomas model.

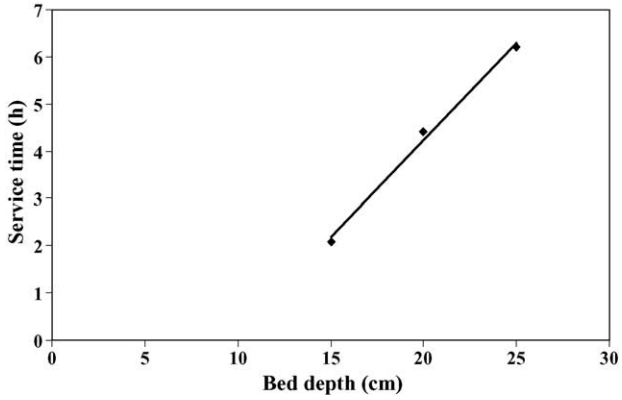

Fig. 5. BDST model plot for AG3 biosorption onto *A. filiculoides*.

simplified design model ignores the intraparticle mass transfer resistance and external film resistance such that the adsorbate is adsorbed onto the adsorbent surface directly. With these assumptions, the BDST model works well and provides useful modeling equations for the changes of system parameters [31]. The column service time was chosen as time when the effluent dye concentration reached 1 mg/L. The plot of service time against bed height at a flow rate of 5 mL/min (Fig. 5) was linear ($R^2 = 0.995$), indicating the validity of BDST model for the present system. The sorption capacity of the bed per unit bed volume, N_0, was calculated from the slope of BDST plot, assuming initial concentration, C_0, and linear velocity, v, as constant during the column operation. The rate constant, K_a, calculated from the intercept of BDST plot, characterizes the rate of solute transfer from the fluid phase to the solid phase [32]. The computed N_0 and

Table 4
Column data and parameters obtained at different bed heights, flow rates and initial dye concentrations

Dye	Bed height (cm)	Flow rate (mL/min)	Inlet dye concentration (mg/L)	t_b (h)	t_e (h)	Uptake (mg/g)	dc/dt (mg/L h)	V_{eff} (L)	Dye removal (%)
AG3	15	5	100	2.1	14.1	50.3	9.52	4.23	58.85
	20	5	100	4.4	19.9	55.8	7.55	5.97	57.40
	25	5	100	6.2	30.2	69.5	4.70	9.06	60.73
	25	10	100	4.6	15.3	66.7	11.12	9.18	57.35
	25	15	100	2.4	9.8	63.6	15.69	8.82	56.93
	25	5	75	8.1	39.8	52.3	2.80	11.79	58.81
	25	5	50	9.2	52.3	65.9	1.37	15.69	52.58

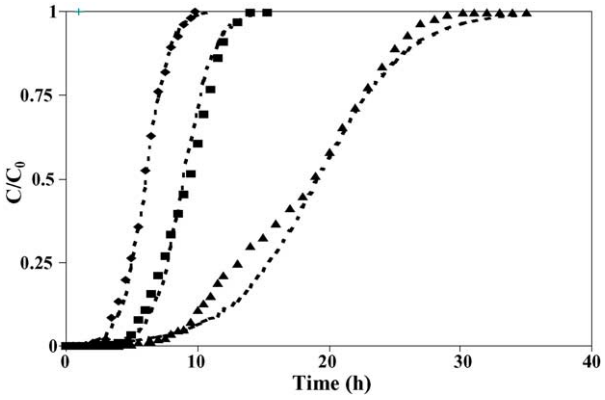

Fig. 6. Breakthrough curves for AG3 biosorption onto *A. filiculoides* biomass at different flow rates (bed height = 25 cm, initial AG3 concentration = 100 mg/L, pH 3.0). Flow rates: (▲) 5 mL/min; (■) 10 mL/min; (♦) 15 mL/min. (- - -) Predicted from Thomas model.

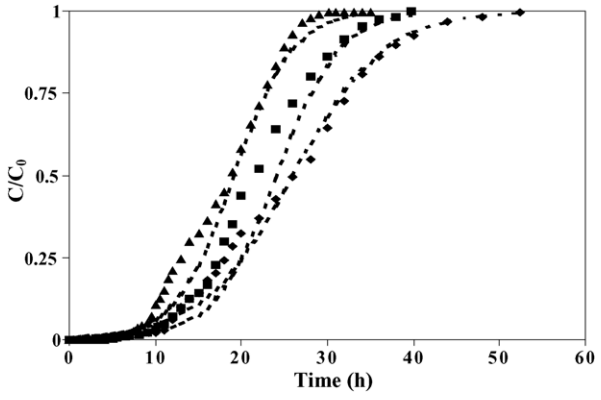

Fig. 7. Breakthrough curves for AG3 biosorption onto *A. filiculoides* biomass at different dye concentrations (bed height = 25 cm, flow rate = 5 mL/min, pH 3.0). Initial dye concentrations: (♦) 50 mg/L; (■) 75 mg/L; (▲) 100 mg/L. (- - -) Predicted from Thomas model.

K_a were 3917 and 0.0116 L/mg h, respectively. The BDST model parameters can be helpful to scale up the process for other flow rates without further experimental run.

3.2.2. Effect of flow rate

Flow rate is one of the important characteristics in evaluating sorbents for continuous-treatment of dyestuff effluents on an industrial scale. The influence of flow rate on the biosorption of AG3 by *A. filiculoides* was investigated by keeping initial dye concentration (100 mg/L) and bed height (25 cm) constant and varying the flow rate from 5 to 15 mL/min (Fig. 6). In contrast to bed height results, the column performed well at lowest flow rate. Earlier breakthrough time appeared at the highest flow rate, resulting in low uptake and least percentage removal. This behavior may be due to insufficient time for the solute inside the column and the diffusion limitations of the solute into the pores of the sorbent at higher flow rates [31].

3.2.3. Effect of initial dye concentration

The biosorption performance of *A. filiculoides* was observed at different inlet dye concentration. The breakthrough curves obtained by changing dye concentration from 50 to 100 mg/L at 5 mL/min flow rate and 25 cm bed height are shown in Fig. 7. A decreased inlet dye concentrations gave delayed breakthrough curves and the treated volume was also higher, since the lower concentration gradient caused slower transport due to decreased diffusion coefficient [21]. At the highest AG3 concentration (100 mg/L) the *Azolla* bed saturated quickly leading to earlier breakthrough and exhaustion time. Table 4, shows that highest uptake and high percentage dye removal are obtained at the highest dye concentration. Also more positive and steep breakthrough curve was obtained for 100 mg dye/L. The driving force for biosorption is the concentration difference between the dye on the biosorbent and the dye in the solution [21]. Thus the high driving force due to the high AG3 concentration resulted in better column performance.

3.2.4. Application of the Thomas model

The Thomas model is one of the most general and widely used models in packed column. The Thomas model, which assumes Langmuir kinetics of adsorption–desorption and no axial dispersion, is derived with the adsorption that the rate driving force obeys second order reversible reaction kinetics. The Thomas model also assumes a constant separation factor but it is applicable to either favorable or unfavorable isotherms [21].

Comparison of experimentally determined and Thomas model predicted breakthrough curves are shown in

Table 5
Thomas model parameters at different conditions

Dye	Bed height (cm)	Flow rate (mL/min)	Inlet dye concentration (mg/L)	Q_{exp} (mg/g)	Q_0 (mg/g)	k_{Th} (L/mg h)	$R^{2\dagger}$
AG3	15	5	100	50.3	51.3	0.0056	0.999
	20	5	100	55.8	54.6	0.0052	0.995
	25	5	100	69.5	72.8	0.0030	0.999
	25	10	100	66.7	69.0	0.0088	0.996
	25	15	100	63.6	68.2	0.0111	0.999
	25	5	75	52.3	68.8	0.0037	0.997
	25	5	50	65.9	49.4	0.0038	0.998

† Correlation coefficient.

Figs. 4, 6 and 7. In general, good fits were obtained in all cases with correlation coefficients ranging from 0.996 to 0.999 for AG3. Table 5 summarizes the Thomas model parameters obtained at different bed heights, flow rates and initial AG3 concentrations. As bed height increased, the values of Q_0 increased and the values of k_{Th} decreased. The bed capacity Q_0 decreased and Thomas constant k_{Th} increased with increasing flow rate. Similarly, Aksu and Gönen [21] observed that as the flow rate increases, the bed capacity decreases and Thomas constant increases for phenol biosorption to Mowital® B30H resin immobilized activated sludge. In contrast, Q_0 increased and k_{Th} decreased with increasing initial AG3 concentration. In most cases, a negligible difference between the experimental (Q_{exp}) and predicted (Q_0) values of the bed capacity was observed.

4. Summary and conclusions

The present study investigated the following features of dye biosorption on deactivated macro blue green fresh water alga *A. filiculoides* in a batch reactor and in a packed bed column.

- The color removal is dependent on initial dye concentration, initial pH and the nature of dye.
- From Langmuir isotherm, as the pH increases the biosorption capacity of AR88 increases and attains maximum value at neutral pH. In the case of AG3 and AO7 the biosorption capacity attains maximum at pH 3.
- On exposing *A. filiculoides* to dye solution, it was observed that most of the process involving dye sorption was completed within 5–6 h followed by a slow process, which leads to the equilibrium dye concentration.
- The kinetics of sorption at a constant biosorption dosage is pseudo second order with the parameters themselves directly varying with dye concentration.
- On comparing the three dyes, *A. filiculoides* exhibited maximum uptake in the case of AG3 in batch experiments and it was selected for the column studies.
- Column experiments were performed in a packed column, as it makes the best use of the concentration difference, which is a driving force for adsorption.
- A series of column studies revealed that bed height, flow rate and initial dye concentration affect AG3 biosorption by *A. filiculoides*. The highest bed height (25 cm), lowest flow rate (5 mL/min) and highest dye concentration (100 mg/L) performed well in AG3 biosorption.
- A successful biosorption process depends on dye uptake performance and continuous supply of biomass. Therefore, it is preferable to use biomass, which is either an industrial waste or available abundance in nature. *A. filiculoides* is one of the most richly available and rapidly reproducing fresh water algae. Also the cultivation method of *A. filiculoides* is trouble-free and also incurred low production cost.
- Thus, *A. filiculoides* possesses all intrinsic characteristics to be employed for the treatment of Acid red 88, Acid green 3 and Acid orange 7 bearing industrial effluents.

References

[1] B.D. Bhole, B. Ganguly, A. Madhuram, D. Deshpande, J. Joshi, Biosorption of methyl violet, basic fuchsin and their mixture using dead fungal biomass, Curr. Sci. 86 (12) (2004) 1641–1645.
[2] C.A. Fewson, Biodegradation of xenobiotic and other persistent compounds: the causes of recalcitrance, Trends Biotechnol. 6 (1988) 148–153.
[3] Y. Fu, T. Viraraghavan, Fungal decolorization of dye wastewater: a review, Bioresour. Technol. 79 (2001) 251–262.
[4] I.M. Banat, P. Nigam, D. Singh, R. Marchant, Microbial decolorization of textile–dye-containing effluents: a review, Bioresour. Technol. 58 (1996) 217–227.
[5] P.C. Vanderviere, R. Bianchi, W. Verstraete, Treatment and reuse of wastewater from the textile wet processing industry: review of emerging technologies, J. Chem. Technol. Biotechnol. 72 (1998) 289–302.
[6] A.F. Strickland, W.S. Perkins, Decolorization of continuous dyeing wastewater by ozonation, Textile Chem. Colorists 27 (5) (1995) 11–15.
[7] Y.S. Ho, G. McKay, Sorption of dye from aqueous solution by peat, Chem. Eng. J. 72 (2) (1998) 115–124.
[8] S. Venkata Mohan, Y. Vijay Bhaskar, J. Karthikeyan, Biological decolorization of simulated azo dye in aqueous phase by algae *Spirogyra* species, Int. J. Environ. Poll. 21 (3) (2003) 211–222.
[9] K.R. Ramakrishna, T. Viraraghavan, Dye removal using low cost adsorbents, Wat. Sci. Technol. 36 (2–3) (1997) 189–196.
[10] Z. Aksu, Reactive dye bioaccumulation by *Saccharomyces cerevisiae*, Proc. Biochem. 38 (10) (2003) 1437–1444.
[11] W.L. Chao, S.L. Lee, Decolorization of azo dyes by three white rot fungi: influence of carbon source, World J. Microbiol. Biotechnol. 10 (1994) 556–559.
[12] R.H.S.F. Vieira, B. Volesky, Biosorption: a solution to pollution? Int. Microbial. 3 (2000) 17–24.
[13] B. Koumanova, P. Peeva, S.J. Allen, K.A. Gallagher, M.G. Healy, Biosorption from aqueous solutions by egg shell membrane and *Rhizopus oryzae*: equilibrium and kinetic studies, J. Chem. Technol. Biotechnol. 77 (2002) 539–545.
[14] Z. Aksu, S. Tezer, Biosorption of reactive dyes on the green alga *Chlorella vulgaris*, Proc. Biochem. 40 (2005) 1347–1361.
[15] E. Acuner, F.B. Dilek, Treatment of tectilon yellow 2 G by *Chorella vulgaris*, Proc. Biochem. 39 (5) (2004) 623–631.
[16] K.T. Semple, R.B. Cain, S. Schmidt, Biodegradation of aromatic compounds by microalgae, FEMS Microb. Lett. 176 (2) (1999) 291–301.
[17] M. Zhao, J.R. Duncan, Batch removal of hexavalent chromium by *Azolla filiculoides*, Appl. Biochem. Biotechnol. 26 (1997) 179–183.
[18] M. Zhao, J.R. Duncan, R.P. Van Hille, Removal and recovery of zinc from solution and electroplating effluent using *Azolla filiculoides*, Wat. Res. 33 (6) (1999) 1516–1522.
[19] M. Zhao, J.R. Duncan, Removal and recovery of nickel from aqueous solution and electroplating rinse effluent using *Azolla filiculoides*, Proc. Biochem. 33 (1998) 249–255.
[20] B. Volesky, J. Weber, J.M. Park, Continuous-flow metal biosorption in a regenerable Sargassum column, Wat. Res. 37 (2003) 297–306.
[21] Z. Aksu, F. Gönen, Biosorption of phenol by immobilized activated sludge in a continuous packed bed: prediction of breakthrough curves, Proc. Biochem. 39 (2003) 599–613.
[22] R.A. Hutchins, New method simplifies design of activated carbon systems, Chem. Eng. 80 (1973) 133–138.

[23] G. Yan, T. Viraraghavan, Heavy metal removal in a biosorption column by immobilized *M. rouxii* biomass, Bioresour. Technol. 78 (2001) 243–249.
[24] P. Waranusantigul, P. Pokethitiyook, M. Kruatrachue, E.S. Upatham, Kinetics of basic dye (methylene blue) biosorption by giant duckweed (*Spirodela polyrrhiza*), Environ. Pollut. 125 (2003) 385–392.
[25] M. Sankar, G. Sekaran, S. Sadulla, T. Ramasami, Removal of diazo and triphenylmethane dyes from aqueous solutions through an adsorption process, J. Chem. Technol. Biotechnol. 74 (1999) 337–344.
[26] I. Langmuir, The adsorption of gases on plane surfaces of glass, mica and platinum, J. Am. Chem. Soc. 40 (1918) 1361–1403.
[27] H. Freundlich, Ueber die adsorption in loesungen, Z. Phys. Chem. 57 (1907) 385–470.
[28] G. McKay, Y.S. Ho, J.C.Y. Ng, Biosorption of copper from waste waters: A review, Sep. Purif. Methods 28 (1999) 87–125.
[29] Z. Zulfadhly, M.D. Mashitah, S. Bhatia, Heavy metals removal in fixed-bed column by the macro fungus *Pycnoporus sanguineus*, Environ. Pollut. 112 (2001) 463–470.
[30] K. Vijayaraghavan, J. Jegan, K. Palanivelu, M. Velan, Removal of nickel(II) ions from aqueous solution using crab shell particles in a packed bed up-flow column, J. Hazard. Mat. 113B (1–3) (2004) 223–230.
[31] D.C.K. Ko, J.F. Porter, G. McKay, Optimised correlations for the fixed-bed adsorption of metal ions on bone char, Chem. Eng. Sci. 55 (2000) 5819–5829.
[32] D.O. Cooney, Adsorption Design for Wastewater Treatment, CRC press, Boca Raton, 1999.